Hindawi Publishing Corporation
Mathematical Problems in Engineering
Volume 2016, Article ID 1932107, 13 pages
http://dx.doi.org/10.1155/2016/1932107

Research Article

Coupling Mechanism and Decoupled Suspension Control Model of a Half Car

Hailong Zhang,[1,2] Ning Zhang,[1] Fuhong Min,[2] Subhash Rakheja,[3] Chunyi Su,[3] and Enrong Wang[2]

[1]*Magneto-Electronic Lab, School of Physics and Technology, Nanjing Normal University, Nanjing 210046, China*
[2]*Vibration Control Lab, School of Electrical and Automation Engineering, Nanjing Normal University, Nanjing 210042, China*
[3]*Center for Advanced Vehicle Engineering, Department of Mechanical Engineering, Concordia University, Montreal, QC, Canada H3G 1M8*

Correspondence should be addressed to Enrong Wang; erwang@njnu.edu.cn

Received 21 November 2015; Revised 3 April 2016; Accepted 6 April 2016

Academic Editor: Reza Jazar

A structure decoupling control strategy of half-car suspension is proposed to fully decouple the system into independent front and rear quarter-car suspensions in this paper. The coupling mechanism of half-car suspension is firstly revealed and formulated with coupled damping force (CDF) in a linear function. Moreover, a novel dual dampers-based controllable quarter-car suspension structure is proposed to realize the independent control of pitch and vertical motions of the half car, in which a newly added controllable damper is suggested to be installed between the lower control arm and connection rod in conventional quarter-car suspension structure. The suggested damper constantly regulates the half-car pitch motion posture in a smooth and steady operation condition meantime achieving the expected completely structure decoupled control of the half-car suspension, by compensating the evolved CDF.

1. Introduction

In the past decade, the active and semiactive control study of intelligent vehicle suspension is a hot topic in international vehicle engineering [1–13], whereas the coordinate control on full-car suspension has become a challenge bottleneck problem and heavily restricts the application and further performance improvement of intelligent suspension, due to strong coupling characteristic among the four quarter-car subsuspensions in a full car. There have been a lot of valuable papers reported in the research of decoupling [14–20]. Reference [14] proposed an ideal output tracking controller to achieve the almost disturbance decoupled control in a half car, by combining both feedback linearization and feedforward neural network control schemes, wherein the suspension inner coupling property was neglected and more undetermined parameters were required to synthesize controller of the MIMO nonlinear system. Reference [15] proposed a controller for decomposing the full-car system into two half-car models under a mild symmetry, and the roll/warp half car was further decomposed into two quarter-cars under a rigor assumed conditions and showed the effectiveness of reducing dive and squat under acceleration and braking. Reference [16] focused on the decoupling and hierarchical vibration control of a 6-DoF half-car suspension, in which there were more presumed conditions and only an approximately decoupled control model was obtained. Reference [17] proposed a human-like intelligent controller by regarding the full car as a quickly moving robot, in which eight poses were classified according to different coupling properties in the full-car vertical, pitch, and roll motions. References [18, 19] proposed a new decoupled control model by decoupling the four quarter-car suspensions in a full car into three quarter-car suspensions, which could greatly simplify the full-car controller synthesis complex and directly apply the proposed ripper control scheme for the quarter-car suspension, whereas the decoupled quarter-car suspension model yielded a large physical change. Reference [20] proposed a simplified measure and vehicle property index to permit a preliminary

evaluation of different interconnected suspension configurations, through using qualitative scaling of the bounce-, roll-, pitch-, and warp-mode stiffness properties, which could offer considerable potential in realizing enhanced decoupling among the different suspension modes. Above-mentioned study results provide ideas for decoupling the subsuspension systems in the full car and achieve an approximation decoupling effect. Yet, until now, still few publications have deeply investigated the coupling mechanism among the multiple quarter-car subsuspension systems in the half and full car, and above-mentioned studies have not achieved an idealized full-structure decoupled suspension control model, composed of the numbered independent quarter-car suspension standard dynamic models in the car. As a result, the proposed coordinate or decoupling control schemes seem more complicate and difficult in real application. The reason is that the studied half- and full-car suspensions are always aimed at the conventional sprung mass damper-based quarter-car suspension structure, even though the linearization technique is utilized for modeling the suspension dynamic system by reasonably ignoring nonlinearities of the damper and car components. However, the established original half- and full-car models are still a complicated asymmetric multiple-input-multiple-output system, from which it is almost impossible to achieve the full-structure decoupled suspension control model, through utilizing the pure mathematical decoupling or advanced control methods.

In this paper, a full-structure decoupling suspension control scheme is originally proposed to decouple the half-car suspension into independent front and rear standard quarter-car suspensions. A 4-DoF half-car suspension dynamic model is firstly established and reorganized in a new formulation involving the front and rear 2-DoF quarter-car suspension models with coupling characteristic, by using a smart mathematical equivalent transformation method. The half-car coupling mechanism between the front and rear quarter-car suspensions is then conveniently revealed and quantitatively formulated with a coupled damping force (CDF). The CDF is an evolved damping force in a linear function of the half-car body pitch angular acceleration and only supplements the front and rear quarter-car suspension damper forces with the same magnitude but an inverse phase. In order to achieve the expected half-car suspension structure decoupled control model, a novel dual dampers-based controllable quarter-car suspension structure is further proposed, by installing another extra controllable damper between the lower control arm and connecting rod in the conventional quarter-car suspension structure. The suggested damper serves function of regulating the half-car body pitch motion posture in a smooth and steady operation condition and meantime fully compensating the evolved CDF, by yielding the damper force in response to the online measured pitch angular acceleration.

The paper is organized as follows. In Section 2, the coupling mechanism of half-car suspension is revealed. In Section 3, dual dampers-based controllable quarter-car suspension structure is introduced for the first time. Further, structure decoupled control model of half-car suspension is analyzed in Section 4; meanwhile the decoupling controller is derived. Section 5 shows the evaluation of the proposed full-structure decoupling control method, by comparing the time and frequency domain responses of the coupling and decoupled half-car suspensions under different conditions. Finally, Section 6 presents the summary and forecast.

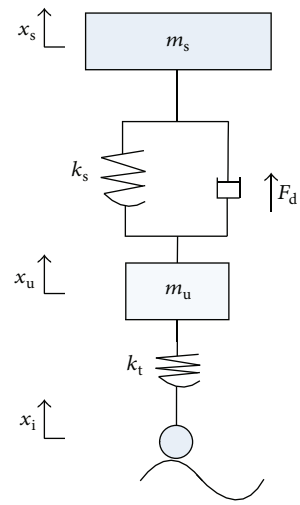

Figure 1: Dynamic model of conventional 2-DoF quarter-car suspension.

2. Coupling Mechanism of Half-Car Suspension

2.1. Conventional 2-DoF Quarter-Car Suspension Model. A common 2-DoF dynamic model of the sprung mass damper-based quarter-car suspension is shown in Figure 1, which is used to study the vertical motion suspension performance of a car by linearizing the associated suspension components. Herein, the damper may be either the conventional passive damper or the active and semiactive controllable dampers, which is generally characterized with F_d for avoiding the damper nonlinearity, m_s and m_u are the sprung and unsprung masses, k_s and k_t are the stiffness of suspension spring and tyre, and x_i, x_s, and x_u are the road excitation and sprung and unsprung mass vertical displacements, respectively. The linearized quarter-car suspension model is formulated as [4–6]

$$\begin{aligned} m_s\ddot{x}_s &= -k_s\left(x_s - x_u\right) - F_d, \\ m_u\ddot{x}_u &= k_s\left(x_s - x_u\right) - k_t\left(x_u - x_i\right) + F_d, \end{aligned} \tag{1}$$

where (1) is considered as the quarter-car suspension standard model, which will play an important role in deriving the half-car suspension full-structure decoupled control model.

2.2. Conventional 4-DoF Half-Car Suspension Model. Figure 2 shows a common 4-DoF half-car suspension dynamic model, involving two front and rear quarter-car suspensions as shown in Figure 1, which is mainly used to study both vertical and pitch motion suspension performances of a car. Herein, M_g, M_{uf}, and M_{ur} express the car body mass and the front and rear quarter-car suspension unsprung masses, J_θ

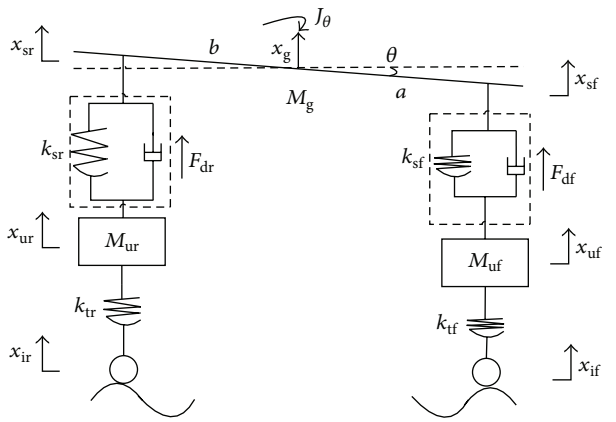

Figure 2: Dynamic model of conventional 4-DoF half-car suspension.

expresses the car body pitch motion inertia, a and b are the front and rear axle distances to the car body center, x_g and θ are the car body vertical motion displacement and pitch motion angle, F_{df} and F_{dr} denote the front and rear quarter-car suspension damper forces, k_{sf}, k_{sr}, k_{tf}, and k_{tr} are stiffness of the front and rear quarter suspension springs and tyres, and x_{sf}, x_{sr}, x_{uf}, x_{ur}, x_{if}, and x_{ir} denote the sprung and unsprung mass vertical displacements and the road excitations of the front and rear quarter-car suspensions, respectively. The linearized half-car suspension model is formulated as [14]

$$M_g\ddot{x}_g + k_{sf}\left(x_{sf} - x_{uf}\right) + k_{sr}\left(x_{sr} - x_{ur}\right) = -F_{df} - F_{dr}, \quad (2)$$

$$J_\theta\ddot{\theta} - ak_{sf}\left(x_{sf} - x_{uf}\right) + bk_{sr}\left(x_{sr} - x_{ur}\right) = aF_{df} - bF_{dr}, \quad (3)$$

$$M_{uf}\ddot{x}_{uf} - k_{sf}\left(x_{sf} - x_{uf}\right) + k_{tf}\left(x_{uf} - x_{if}\right) = F_{df}, \quad (4)$$

$$M_{ur}\ddot{x}_{ur} - k_{sr}\left(x_{sr} - x_{ur}\right) + k_{tr}\left(x_{ur} - x_{ir}\right) = F_{dr}. \quad (5)$$

The dynamic properties of half-car body vertical and pitch motions are formulated in (2)–(5), as well as unsprung mass vertical motions in front and rear quarter-car suspensions, respectively.

By subtracting (2) multiplied by b and (3) and subtracting (2) multiplied by a and (3), respectively, we obtain

$$\begin{aligned} bM_g\ddot{x}_g - J_\theta\ddot{\theta} + k_{sf}(a+b)\left(x_{sf} - x_{uf}\right) &= -(a+b)F_{df}, \\ aM_g\ddot{x}_g + J_\theta\ddot{\theta} + k_{sr}(a+b)\left(x_{sr} - x_{ur}\right) &= -(a+b)F_{dr}. \end{aligned} \quad (6)$$

Since the magnitude of pitch angle θ is usually a small value, the vertical sprung mass displacements in front and rear quarter-car suspensions can be thus approximately expressed as

$$\begin{aligned} x_g &= x_{sf} + a\theta, \\ x_g &= x_{sr} - b\theta. \end{aligned} \quad (7)$$

Substituting (7) into (6) leads to

$$\begin{aligned} \frac{b}{a+b}M_g\ddot{x}_{sf} &= -k_{sf}\left(x_{sf} - x_{uf}\right) - F_{df} \\ &\quad - \left(\frac{ab}{a+b}M_g - \frac{J_\theta}{a+b}\right)\ddot{\theta}, \\ \frac{a}{a+b}M_g\ddot{x}_{sr} &= -k_{sr}\left(x_{sr} - x_{ur}\right) - F_{dr} \\ &\quad + \left(\frac{ab}{a+b}M_g - \frac{J_\theta}{a+b}\right)\ddot{\theta}, \end{aligned} \quad (8)$$

where we denote $M_{sf} = (b/(a+b))M_g$ and $M_{sr} = (a/(a+b))M_g$, which just represent the sprung masses of front and rear quarter-car suspensions in the half-car, respectively.

We further set

$$F_{sf} = F_{df} + F_c\left(\ddot{\theta}\right), \quad (9)$$

$$F_{sr} = F_{dr} - F_c\left(\ddot{\theta}\right), \quad (10)$$

$$F_c\left(\ddot{\theta}\right) = K_c\ddot{\theta}, \quad (11)$$

$$K_c = \frac{ab}{a+b}M_g - \frac{J_\theta}{a+b}. \quad (12)$$

By replacing (9)–(12) with (8) and combining with (4) and (5), we obtain a new half-car suspension dynamic model as follows:

$$\begin{aligned} M_{sf}\ddot{x}_{sf} &= -k_{sf}\left(x_{sf} - x_{uf}\right) - F_{sf}, \\ M_{uf}\ddot{x}_{uf} &= k_{sf}\left(x_{sf} - x_{uf}\right) - k_{tf}\left(x_{uf} - x_{if}\right) + F_{df}, \end{aligned} \quad (13)$$

$$\begin{aligned} M_{sr}\ddot{x}_{sr} &= -k_{sr}\left(x_{sr} - x_{ur}\right) - F_{sr}, \\ M_{ur}\ddot{x}_{ur} &= k_{sr}\left(x_{sr} - x_{ur}\right) - k_{tr}\left(x_{ur} - x_{ir}\right) + F_{dr}. \end{aligned} \quad (14)$$

The half-car front and rear quarter-car suspension dynamic models with coupling characteristic are formulated in (14) and (15), respectively, because they are quite similar to the standard dynamic model of quarter-car suspension given by (1), in which the only difference embodies the evolved coupling term $F_c(\ddot{\theta})$ shown in (10) and (11). It is easily found that $F_c(\ddot{\theta})$ quantitatively expresses the coupling characteristic between the front and rear quarter-car suspensions in half-car; for further discovering the half-car suspension coupling mechanism, we name $F_c(\ddot{\theta})$ and K_c as the coupled damping force (CDF) and the coupling coefficient, respectively. Moreover, (12) shows that $F_c(\ddot{\theta})$ is an evolved suspension damping force being a linear function of the half-car body pitch angular acceleration $\ddot{\theta}$ and only supplements the yielded front and rear quarter-car suspension damper forces with the same magnitude but an inverse phase. Equation (13) further shows that K_c is a constant ratio of $F_c(\ddot{\theta})$ to $\ddot{\theta}$, subject to four parameters (M_g, J_θ, a, and b) of a car design.

2.3. Coupling Mechanism of Half-Car Suspension. Consider the following:

(i) From (9) and (10), it is found that the half-car front and rear total suspension damping forces (F_{sf}, F_{sr})

are superposition of the yielded damper forces (F_{df}, F_{dr}) and the evolved CDF ($F_c(\ddot{\theta})$) with the same magnitude but an inverse phase, which means that if F_{sf} increases, then F_{sr} decreases and vice versa.

(ii) Equation (11) shows that if $\ddot{\theta} = 0$, then $F_c(\ddot{\theta}) = 0$, which illustrates that when the car moves on an ideally smooth road, the half-car body pitch motion will never occur and its front and rear quarter-car suspensions are mutually independent. In this case, the half-car suspension model, given by (13) and (14), can be easily simplified as the independent front and rear quarter-car suspension standard models. It is just the reason that the quarter-car suspension has been widely employed for the vehicle vertical motion suspension study by international scholars.

(iii) Equation (11) further shows that if $\ddot{\theta} \neq 0$ and $K_c \neq 0$, then $F_c(\ddot{\theta}) \neq 0$, it is said that when the car moves on a rough road, the half-car body pitch motion and coupling of front and rear quarter-car suspensions will inevitably occur, and this means that the half-car body pitch motion is the essential cause leading to coupling characteristic between the front and rear quarter-car suspensions. Moreover, the coupled serious degree mainly depends on the magnitude of coupling coefficient K_c, in which an idealized case is that if $K_c = 0$, the half-car suspension coupling will still never occur, even if the car moves on a quite rough road, whereas (12) shows that letting $K_c = 0$ is rarely impossible, and one can only make K_c a small value, by reasonably modifying the associated car design parameters.

(iv) In a car normal moving case such as $\ddot{\theta} \neq 0$, $K_c \neq 0$, and $F_c(\ddot{\theta}) \neq 0$, (13) and (14) further show that $F_c(\ddot{\theta})$ may be fully compensated, by artificially adding a control force (F_{uf}, F_{ur}) in both front and rear unsprung mass motion equations and making $F_{uf} = F_c(\ddot{\theta})$ and $F_{ur} = -F_c(\ddot{\theta})$, such that $F_{sf} = F_{df} + F_{uf}$ and $F_{sr} = F_{dr} + F_{ur}$, which means that (13) and (14) can be equivalently transferred to the independent front and rear quarter-car suspension standard models. The proposed decoupling control scheme of half-car suspension exhibits a clear physical meaning of indirectly eliminating the suspension coupling characteristic, by effectively regulating the half-car pitch motion posture in a smooth and steady operation condition.

3. Dual Dampers-Based Controllable Quarter-Car Suspension Structure

In order to physically realize the above-proposed half-car suspension decoupling control scheme, that is, adding control forces (F_{uf}, F_{ur}) in the unsprung mass motion equations of half-car front and rear quarter-car suspensions and making $F_{uf} = F_c(\ddot{\theta})$ and $F_{ur} = -F_c(\ddot{\theta})$, respectively, a novel dual dampers-based controllable quarter-car suspension structure is initially proposed as shown in Figure 3. Herein, the original

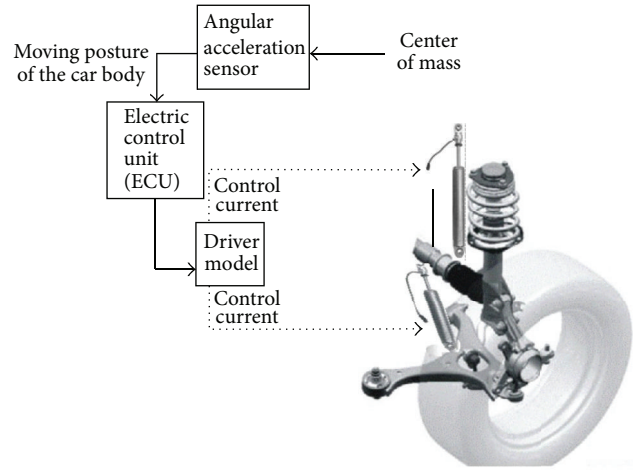

Figure 3: Dual dampers-based controllable quarter-car suspension structure.

sprung mass suspension damper is reserved for controlling the car vertical motion suspension performance, while another unsprung mass controllable damper is suggested to be installed between the low control arm and control rod almost in parallel with the wheel [21], so as to control the half-car body pitch motion posture in smooth and steady operation condition. Moreover, a decoupling control unit, including the angular acceleration sensor and controller, is acquired to generate the front and rear unsprung mass damper forces (F_{uf}, F_{ur}) in response to the online measured half-car body pitch angle acceleration ($\ddot{\theta}$). The proposed dual dampers-based controllable quarter-car suspension structure merits easy engineering implementation, due to maintaining the original sprung mass-based quarter-car suspension structure [22].

The dynamic model of the proposed dual dampers-based controllable quarter-car suspension structure, as shown in Figure 3, can be conveniently established in (15), by employing the same modeling way and model parameter variables for the conventional quarter-car suspension given by (1), in which the only difference is adding a term of the unsprung mass damper force (F_u) in the unsprung mass motion equation, by comparing (15) with (1). It is easily found that the conventional sprung mass-based and novel dual dampers-based quarter-car suspensions are the same, when $F_u = 0$:

$$\begin{aligned} m_s\ddot{x}_s &= -k_s(x_s - x_u) - F_d, \\ m_u\ddot{x}_u &= k_s(x_s - x_u) - k_t(x_u - x_i) + F_d + F_u. \end{aligned} \tag{15}$$

4. Structure Decoupled Control Model of Half-Car Suspension

Figure 5 shows the controllable half-car suspension dynamic model, based upon the proposed dual dampers-based controllable quarter-car suspension structure shown in Figure 4, and its model is established in (16), by employing the same

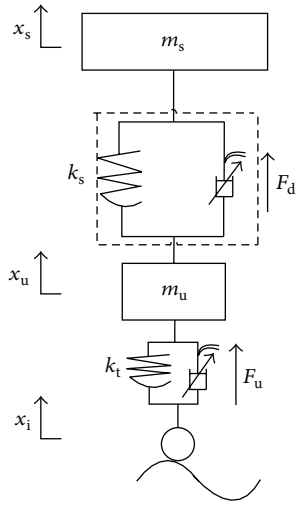

Figure 4: Dynamic model of the dual dampers-based controllable quarter-car suspension.

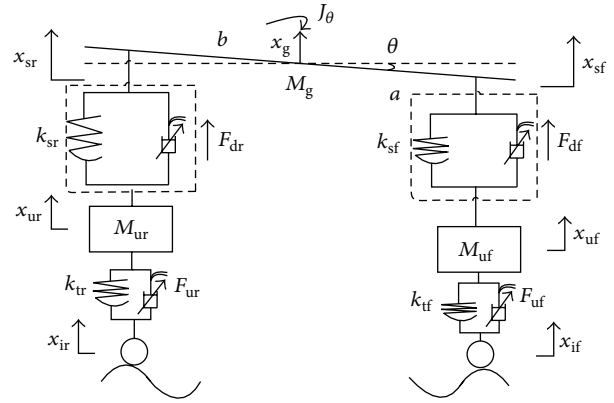

Figure 5: Dynamic model of dual dampers-based controllable half-car suspension.

modeling way and model parameter variables for the conventional half-car suspension given by (2)–(5), in which the only difference is adding the term of unsprung mass damper forces (F_{uf}, F_{ur}) in its unsprung mass motion equations

$$\begin{aligned} M_g\ddot{x}_g &= -k_{sf}\left(x_{sf}-x_{uf}\right)-k_{sr}\left(x_{sr}-x_{ur}\right)-F_{df} \\ &\quad -F_{dr}, \\ J_\theta\ddot{\theta} &= ak_{sf}\left(x_{sf}-x_{uf}\right)-bk_{sr}\left(x_{sr}-x_{ur}\right)+aF_{df} \\ &\quad -bF_{dr}, \\ M_{uf}\ddot{x}_{uf} &= k_{sf}\left(x_{sf}-x_{uf}\right)-k_{tf}\left(x_{uf}-x_{if}\right)+F_{df}+F_{uf}, \\ M_{ur}\ddot{x}_{ur} &= k_{sr}\left(x_{sr}-x_{ur}\right)-k_{tr}\left(x_{ur}-x_{ir}\right)+F_{dr}+F_{ur}. \end{aligned} \tag{16}$$

Furthermore, the similarly decoupled half-car suspension model in (17) is derived from (16), by employing the same mathematical transformation method in Section 2.2. This model is composed of the dual dampers-based controllable full-car front and rear quarter-car suspension models coupled with $F_c(\ddot{\theta})$. By comparing (17) with (13) and (14), it is found that the only difference is adding term of unsprung mass damper forces (F_{uf}, F_{ur}) in their unsprung mass motion equations

$$\begin{aligned} M_{sf}\ddot{x}_{sf} &= -k_{sf}\left(x_{sf}-x_{uf}\right)-F_{df}-F_c\left(\ddot{\theta}\right), \\ M_{uf}\ddot{x}_{uf} &= k_{sf}\left(x_{sf}-x_{uf}\right)-k_{tf}\left(x_{uf}-x_{if}\right)+F_{df}+F_{uf}, \\ M_{sr}\ddot{x}_{sr} &= -k_{sr}\left(x_{sr}-x_{ur}\right)-F_{dr}+F_c\left(\ddot{\theta}\right), \\ M_{ur}\ddot{x}_{ur} &= k_{sr}\left(x_{sr}-x_{ur}\right)-k_{tr}\left(x_{ur}-x_{ir}\right)+F_{dr}+F_{ur}. \end{aligned} \tag{17}$$

To achieve the half-car decoupled suspension control model, it is required to realize $F_{uf} = F_c(\ddot{\theta})$ and $F_{ur} = -F_c(\ddot{\theta})$ by synthesizing a decoupling controller. Then the model given by (17) can be rewritten as the decoupled form in (18), which is composed of independent front and rear quarter-car suspension standard models:

$$\begin{aligned} M_{sf}\ddot{x}_{sf} &= -k_{sf}\left(x_{sf}-x_{uf}\right)-F_{sf}, \\ M_{uf}\ddot{x}_{uf} &= k_{sf}\left(x_{sf}-x_{uf}\right)-k_{tf}\left(x_{uf}-x_{if}\right)+F_{sf}, \\ M_{sr}\ddot{x}_{sr} &= -k_{sr}\left(x_{sr}-x_{ur}\right)-F_{sr}, \\ M_{ur}\ddot{x}_{ur} &= k_{sr}\left(x_{sr}-x_{ur}\right)-k_{tr}\left(x_{ur}-x_{ir}\right)+F_{sr}. \end{aligned} \tag{18}$$

With the help of above-mentioned decoupling control scheme, the half-car suspension can be ideally decoupled into two independent front and rear quarter-car suspensions by fully compensating the evolved $F_c(\ddot{\theta})$. For this purpose, the key work is to synthesize a decoupled controller as below:

$$F_{uf} = -F_{ur} = K_c\ddot{\theta}, \tag{19}$$

where the decoupled controller gain is just the proposed coupling coefficient defined in Section 2.1.

5. Evaluation of the Proposed Full-Structure Decoupling Control Method

To verify the correctness of the proposed half-car suspension full-structure decoupling control method, a simulation platform for both coupling and decoupled half-car suspension dynamic systems is built up. The responses of coupling and decoupled half-car suspensions are thoroughly compared under harmonic and rounded pulse excitations inserted on a single tyre, and the employed half-car suspension model parameters are listed in Table 1 [14]. It should be noticed that the passive dampers (C_{sf}, C_{sr}) are employed as the sprung mass suspension dampers, and the added unsprung mass controllable damper forces are generally characterized with F_{uf} and F_{ur} in this study.

5.1. Coupling Characteristic of Conventional Half-Car Suspension. The half-car suspension coupling characteristic is firstly analyzed to evaluate correctness of the proposed coupling mechanism between the half-car front and rear quarter-car suspensions. According to (12) and parameters listed in

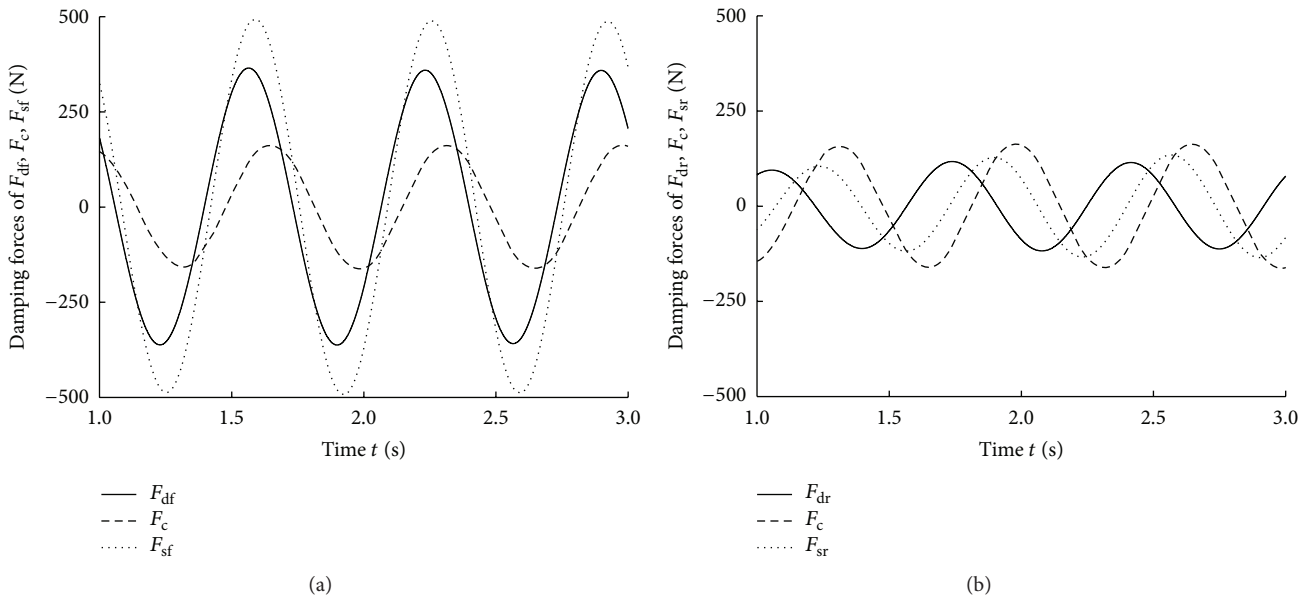

Figure 6: The coupling characteristic of conventional half-car suspension system. (a) Damping forces in front quarter-car suspension. (b) Damping forces in rear quarter-car suspension.

Table 1: Model parameters of the half-car suspension system.

Symbol	Quantity	Value
M_g	Car body mass	575 kg
J_θ	Car body pitch inertia	769 kg·m^2
M_{uf}	Front unsprung mass	60 kg
M_{ur}	Rear unsprung mass	60 kg
k_{tf}	Front tyre stiffness	190 kN/m
k_{tr}	Rear tyre stiffness	190 kN/m
k_{sf}	Front suspension stiffness	16.812 kN/m
k_{sr}	Rear suspension stiffness	16.812 kN/m
C_{sf}	Front damper coefficient	1.0 kN·s/m
C_{sr}	Rear damper coefficient	1.0 kN·s/m
a	Front axle distance to car body center	1.38 m
b	Rear axle distance to car body center	1.36 m

Table 1, the half-car suspension coupling coefficient, that is, the decoupled controller gain, is calculated as $K_c = 113.2$. The conventional half-car suspension, as shown in Figure 2, is analyzed under a harmonic excitation with amplitude 2.5 cm at 1.5 Hz of the half-car sprung mass resonant frequency, which is inserted on the front tyre (x_{if}). Figure 6 illustrates response comparisons of total suspension damping forces (F_{sf}, F_{sr}), damper forces (F_{df}, F_{dr}), and coupled damping force (F_c) in the half-car front and rear quarter-car suspensions. The results clearly show that the magnitude of F_{sf} is much larger than that of F_{sr}, due to the harmonic excitation inserted only on the front tyre. The slight vibration of rear quarter-car suspension that occurred, as shown in Figure 6(b), is the suspension coupling effect transmitted from the front quarter-car suspension, although no excitation is inserted on the rear tyre ($x_{ir} = 0$). Moreover, F_{sf} and F_{sr} are larger and lower than their F_{df} and F_{dr}, because they are superposed by $F_c(\ddot{\theta})$ on F_{df} and F_{dr} with the same magnitude but an inverse phase, respectively. It is obvious that the total suspension damping forces of half-car front and rear quarter-car suspensions are not offered purely by the yielded suspension damper forces, due to the coupling characteristic defined by F_c.

5.2. Frequency Domain Response Analysis of Decoupled Half-Car Suspension. The frequency domain response analysis is an important tool for evaluating vehicle suspension performance due to the larger dominant frequency band 0–20 Hz of road vehicle [2]. For evaluating engineering feasibility of the proposed novel dual dampers-based controllable quarter-car suspension structure, frequency responses of the decoupled half-car suspension are thoroughly compared with those of the conventional coupling half-car suspension based on sprung mass damper-based quarter-car structure. Herein, the evaluation indexes are selected as half-car body center vertical displacement acceleration transmissibility (T_g), sprung mass vertical displacement acceleration transmissibility (T_{sf}, T_{sr}) and dynamic travel transmissibility (T_{df}, T_{dr}) of the front and rear quarter-car suspensions, and Root-Mean-Square (RMS) of the half-car body pitch angular acceleration (a_θ); the calculation method is given in [7].

Figure 7 illustrates the frequency domain response comparisons of both coupling and decoupled half-car suspensions, under discrete harmonic excitations inserted on the front tyre in frequency range 0–20 Hz. The results show that the suggested unsprung mass dampers in the decoupled half-car suspension yield obvious regulation role of the smooth and steady pitch motion posture, due to its much lower RMS magnitudes of a_θ than those of the conventional coupling half-car suspension as shown in Figure 7(b), and realize the expected half-car full-structure decoupling suspension

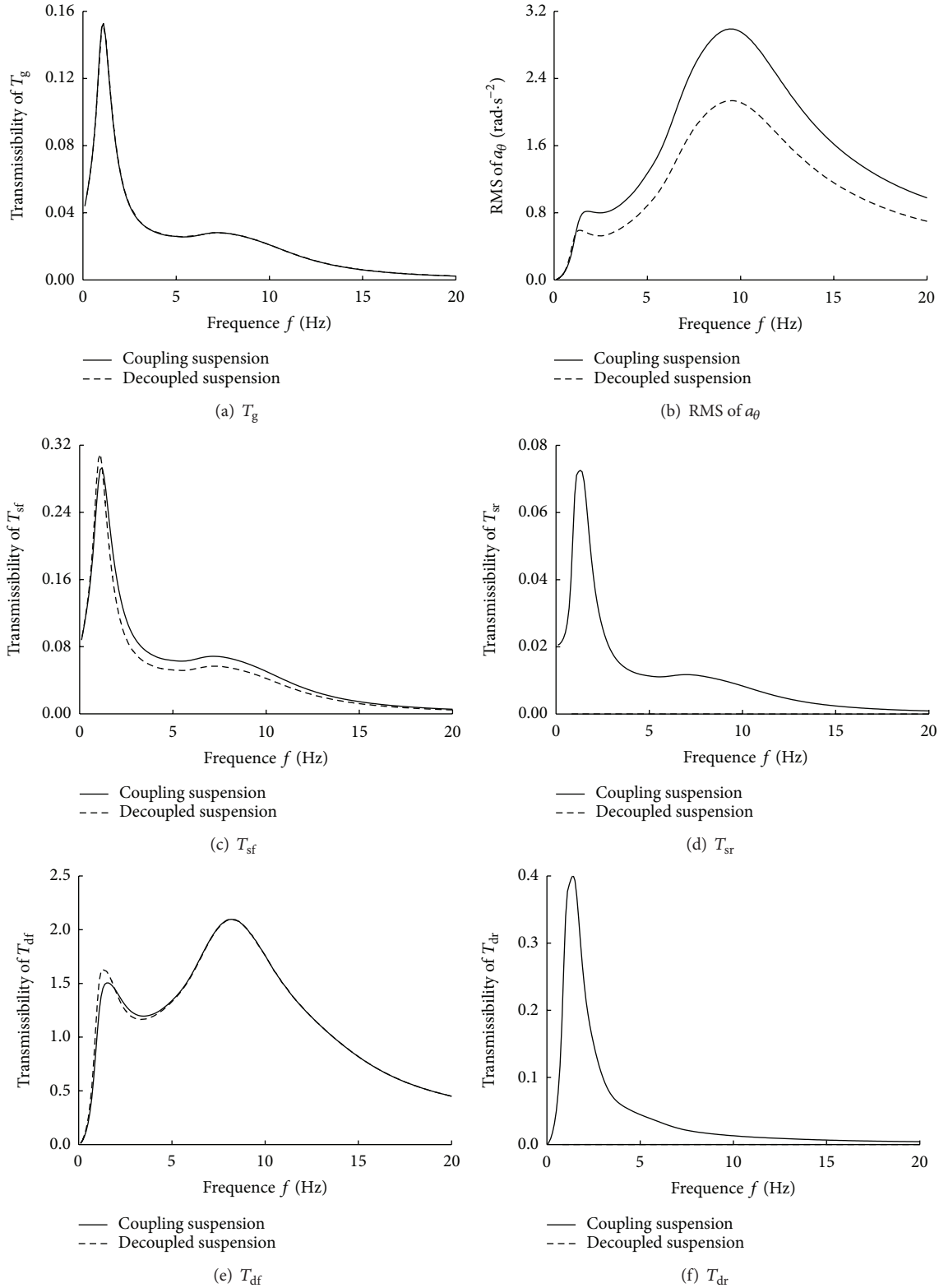

FIGURE 7: Frequency domain response comparisons of coupling and decoupled half-car suspensions: (a) acceleration transmissibility of half-car body center T_g; (b) RMS of pitch angular acceleration a_θ; (c) acceleration transmissibility of front quarter-car suspension T_{sf}; (d) acceleration transmissibility of rear quarter-car suspension T_{sr}; (e) travel transmissibility of front quarter-car suspension T_{df}; and (f) travel transmissibility of rear quarter-car suspension T_{dr}.

control function, because the rear quarter-car suspension of decoupled half-car does not work as shown in Figures 7(d) and 7(f), while the rear quarter-car suspension of coupling half-car still occurs with slight vibration due to the transmitted suspension coupling effect from its front quarter-car suspension, although nonexcitation is inserted on the rear tyre ($x_{ir} = 0$). Moreover, for both coupling and decoupled half-car suspensions, T_g does not change any more as shown in Figure 7(a). Slight vibrations of only T_{sf} and T_{df} do occur as shown in Figures 7(c) and 7(e), which means that the proposed dual dampers-based quarter-car suspension structure does not affect the fundamental vehicle suspension performance, while contributing to develop a new half-car suspension full-structure decoupled control model.

5.3. Evaluation of Half-Car Suspension Full-Structure Decoupled Control Model. The time domain response comparisons of the coupling and decoupled half-car suspensions are further conducted, under a rounded pulse excitation inserted on the front tyre and meantime zero excitation inserted on the rear tyre, given by (20). The employed rounded pulse excitation is used to emulate the usually encountered harsh road surfaces such as hills and hollows, which makes the car body pitch serious. The evaluation indexes are selected as the half-car body center vertical displacement and pitch angular accelerations (a_g, a_θ), the sprung mass displacement accelerations (a_{sf}, a_{sr}), and dynamic travels (x_{df}, x_{dr}) of front and rear quarter-car suspensions, respectively [7]:

$$x_{if} = 0.25 a_m e^2 \left(\mu\omega_0 t\right)^2 e^{-\mu\omega_0 t}, \quad x_{ir} = 0, \tag{20}$$

where parameters of the rounded pulse excitation are chosen as amplitude $a_m = 2.0$ cm, fundamental harmonic frequency $\omega_0 = 10.4$ rad/s, and pulse stiffness $\mu = 3$.

Figure 8 shows the time domain response comparisons of both coupling and decoupled half-car suspensions, under the rounded pulse excitation inserted on front tyre. It is found that a_g remains the same, while magnitudes of a_θ of the decoupled half-car suspension are obviously lower than those of the coupling half-car suspension, as shown in Figures 8(a) and 8(b). The results maintain identical tendency as shown in Figures 7(a) and 7(b), due to the achieved ideal regulation role of half-car body pitch motion posture in smooth and steady operation condition. Furthermore, effectiveness of the proposed half-car suspension decoupled control model can be well verified by comparing the responses of front and rear quarter-car suspensions, as shown in Figures 8(c)–8(f), in which the magnitudes of a_{sf} and x_{df} show only slight variations for both coupling and decoupled front quarter-car suspensions, while the magnitudes of a_{sr} and x_{dr} show quite obvious difference with larger and zero values for the coupling and decoupled front quarter-car suspensions, respectively, because the coupling half-car suspension inevitably transmits vibration from the front quarter-car suspension to the rear quarter-car suspension, while the decoupled half-car suspension has effectively eliminated the coupling characteristic between the half-car front and rear quarter-car suspensions.

5.4. Exploratory Research on the Semiactive Decoupling. In Sections 5.1–5.3, all the results are based on the assumption that the unsprung mass damper provides the active force for fully compensating the CDF. If the unsprung mass damper is a semiactive damper, there may be some problems in the dynamic equations of the suspension, for the reason that the semiactive damper cannot provide the active force and can only dissipate vibration energy. In this section, we intend to discuss the results of the decoupling with magnetorheological damper (MRD), which is known as a classic semiactive damper.

The MRD is certainly able to provide variable damping coefficient rather than wanted active force. Despite that, the desired forces of the front and rear unsprung mass damper are just the opposite at the same time from (19). If one of two unsprung mass dampers serves the desired force with specific driven current, while the other one is working at zero driven current at the same time, we think that an approximate decoupling control is achieved by partly compensating the CDF. Next, the experimental study is carried out to validate the idea. We build up the dedicated semiphysical experiment platform, using hardware-in-the-loop (HIL) simulation technology [23, 24]. Nonphysical model is built in real-time simulation platform with virtual components, including m_s, m_u, k_s, k_t, and x_i. For the restrictions in experimental conditions, the front unsprung mass damper uses the real MRD, while the rear unsprung mass damper uses the modified Bouc-Wen model identified from the real MRD, as shown in Figure 9. The modified Bouc-Wen model structure and parameters are elaborated in [25]. F_{uf} is the actual damping force, and F_{ur} is the calculated damping force of the Bouc-Wen model. The schematic of the experimental set-up is illustrated in Figure 10, where the instruments are numbered from 1 to 11. The platform is composed of four sections, namely, real-time simulation platform (1, 2), MR damper (8), vibration system (3–7), and an interface circuit (10).

In accordance with the analysis in Section 5.3, the smooth pulse is used as road excitation, which is only inserted on the front tyre, given by (20). The system responses are selected as a_g and a_θ a_{sf} and x_{df} a_{sr} and x_{dr}. The results of semidecoupled suspension with MRD are shown by comparing with coupling and decoupled suspensions in Figure 11. Obviously shown in Figures 11(a) and 11(b), the amplitude of both a_g and a_θ of the semiactive decoupled suspension reduces significantly, which is quite different from those of the full-decoupled suspension. It is also found that stabilization time delays by about 0.3 s due to regulation of the driven current for MRD. As shown in Figures 11(c) and 11(e), the vibration amplitude of the front suspension response of the semidecoupled suspension reduces, while the stabilization time also delays by about 0.3 s. We should note that the starting nonlinear oscillations are suppressed effectively in the semidecoupled suspension. By observing the rear suspension system with no excitation, as shown in Figures 11(d) and 11(f), it is found that the suspension vibration is significantly weakened compared with the coupling suspension by partly compensating the CDF though not excellent as the full-decoupled suspension. In conclusion, the semidecoupled

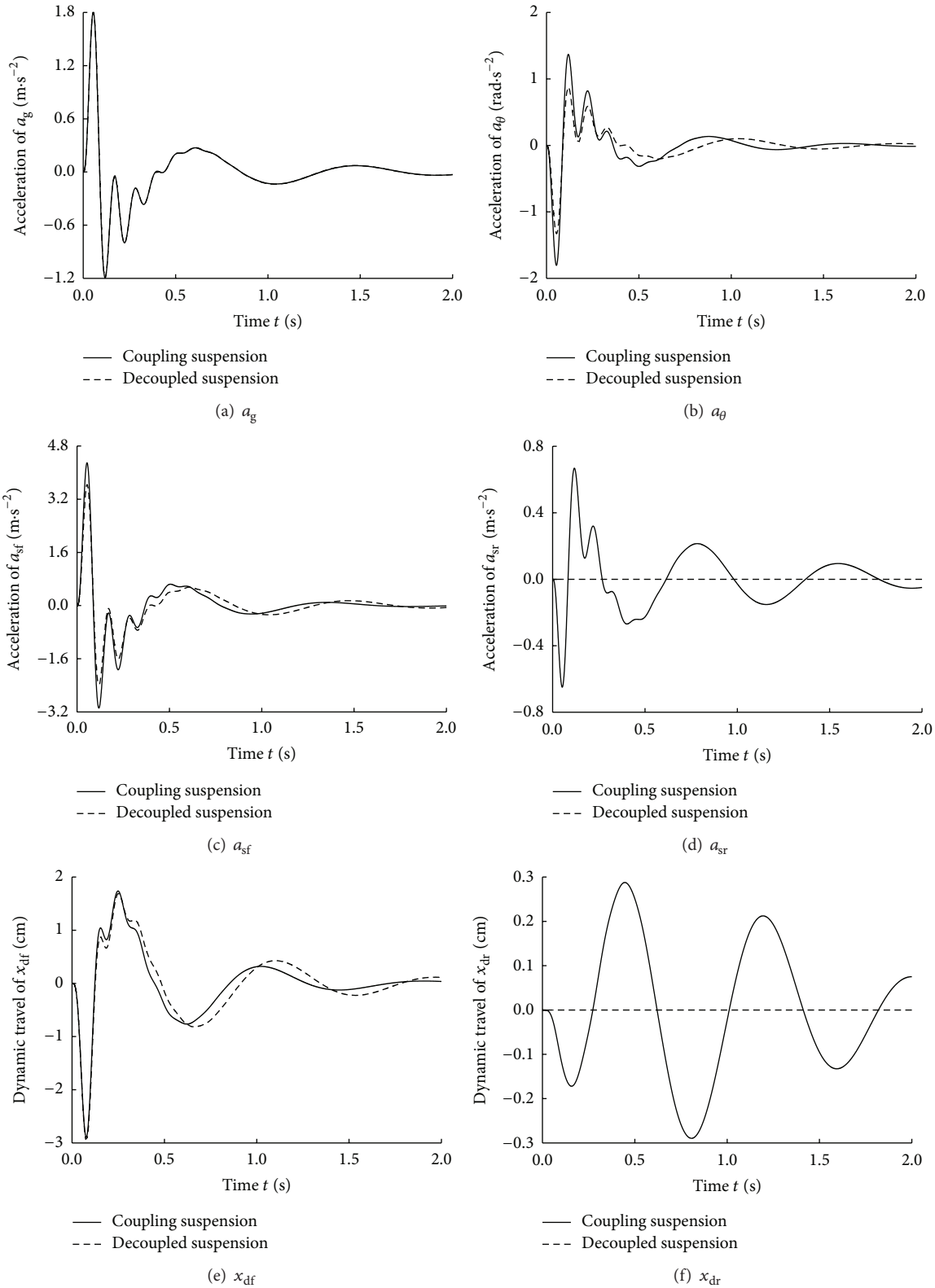

FIGURE 8: Time domain response comparisons of coupling and decoupled half-car suspensions: (a) acceleration of half-car body center a_g; (b) pitch angular acceleration a_θ; (c) acceleration of front quarter-car suspension a_{sf}; (d) acceleration of rear quarter-car suspension a_{sr}; (e) travel displacement of front quarter-car suspension x_{df}; and (f) travel displacement of rear quarter-car suspension x_{dr}.

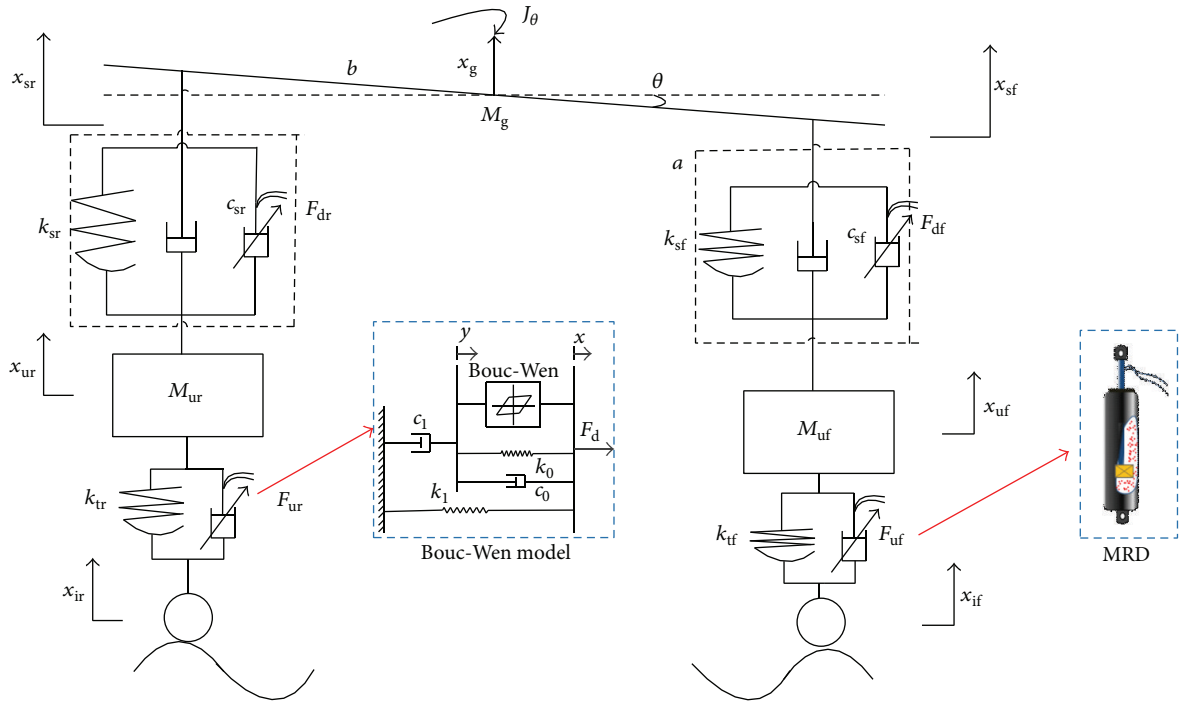

Figure 9: Test sketch of decoupling control of the half car with semiactive damper.

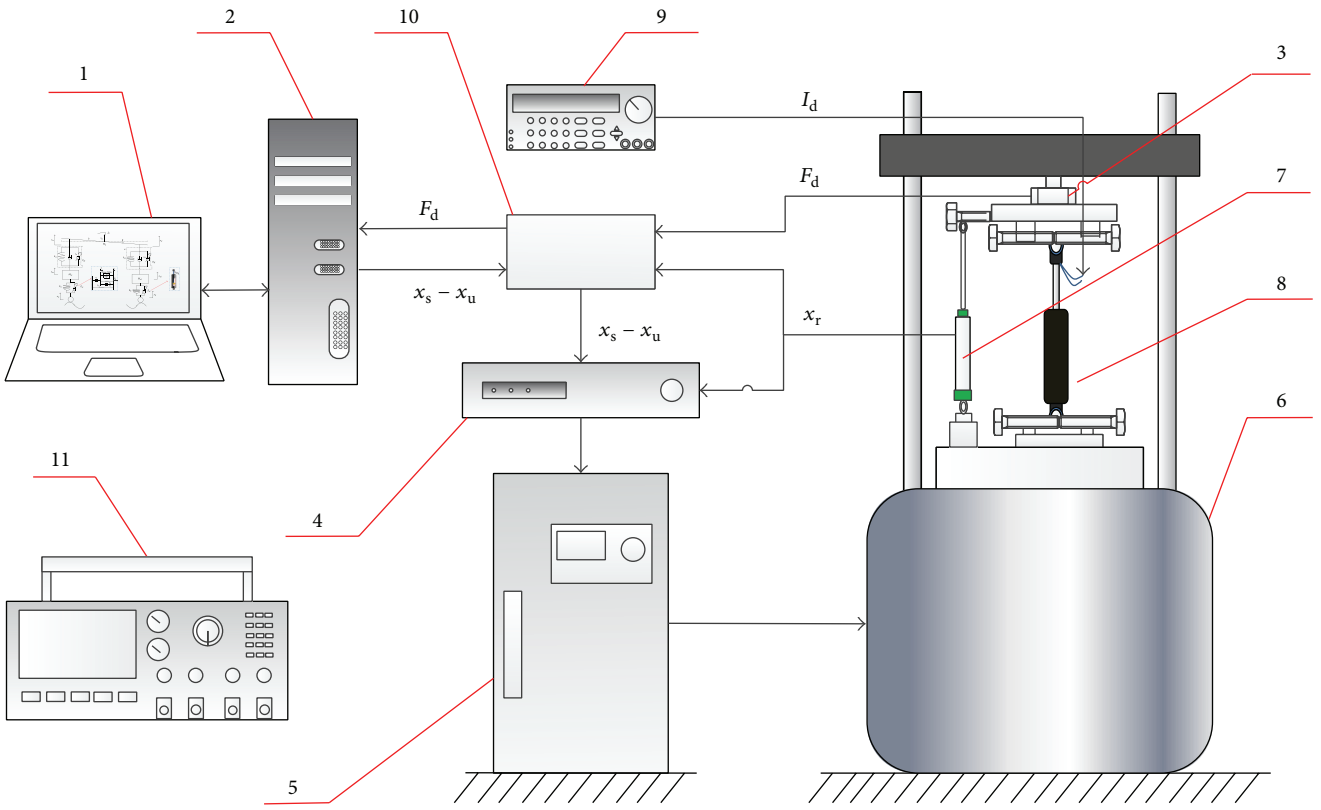

Figure 10: Schematic diagram of the HIL experiment platform (1-personal computer (PC), 2-industrial PC (IPC) with a data acquisition card (DAQC), 3-the load cell, 4-shaker controller, 5-power amplifier, 6-electromagnetic vibration shaker, 7-linear variable differential transformer, 8-MRD, 9-high precision programable power source, 10-interface circuit, and 11-mixed domain digitizing oscilloscope).

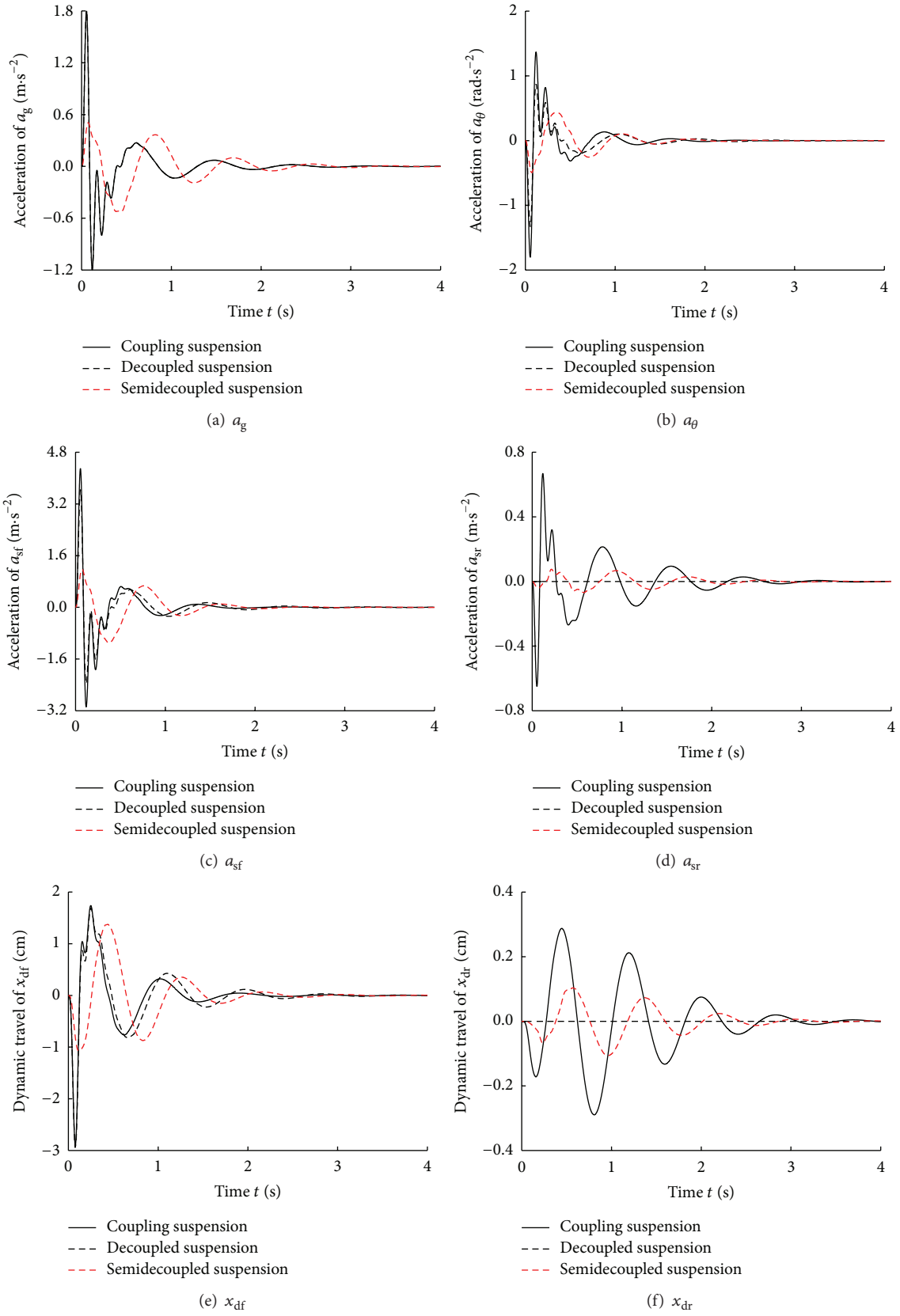

Figure 11: Time domain response comparisons of coupling, decoupled, and semidecoupled half-car suspensions: (a) acceleration of half-car body center a_g; (b) pitch angular acceleration a_θ; (c) acceleration of front quarter-car suspension a_{sf}; (d) acceleration of rear quarter-car suspension a_{sr}; (e) travel displacement of front quarter-car suspension x_{df}; and (f) travel displacement of rear quarter-car suspension x_{dr}.

suspension with semiactive damper such as MRD exhibits a better performance than coupling suspension by partly decoupling.

6. Conclusions

Consider the following:

(1) The coupling mechanism between the half-car front and rear quarter-car suspensions has been originally revealed and quantitatively formulated by the coupled damping force (CDF), which is a linear function of the pitch angular acceleration with a constant ratio of the defined coupling coefficient. The half-car pitch motion is the main cause leading to the coupling characteristic.

(2) A novel dual dampers-based controllable quarter-car suspension structure was originally proposed by installing an unsprung mass controllable damper between the conventional quarter-car suspension lower control arm and connecting rod, which serves function of regulating the half-car pitch motion posture in a smooth and steady operation condition and merits clear physics meaning and easy implementation.

(3) A novel half-car suspension full-structure decoupled control model, composed of independent front and rear standard quarter-car models, was originally proposed, on the basis of the proposed novel dual dampers-based controllable quarter-car suspension structure. A controller is synthesized to decouple the half-car suspension into independent front and rear quarter-car suspensions, by controlling the yielded unsprung mass damper forces in response to the online measured pitch angular acceleration.

(4) The proposed half-car suspension full-structure decoupled control model will put forth a greatly simplified control scheme for realizing the intelligent full-car suspension. The suggested unsprung mass controllable dampers are used to control the half-car pitch motion suspension performance and meantime achieve the half-car suspension full-structure decoupled control model, while the original sprung mass controllable dampers are used to control the decoupled front and rear quarter-car vertical motion suspension performances, respectively.

(5) The selection of the unsprung mass damper is discussed. The active damper can guarantee the supply of the desired force for full decoupling. More generally, the semidecoupled suspension with semiactive MRD as unsprung mass damper is analyzed. The HIL experiment is conducted, and the results show that the semidecoupled suspension also exhibits a good decoupling performance by partly compensating the CDF.

Competing Interests

The authors declare that there is no conflict of interests regarding the publication of this paper.

Acknowledgments

The research leading to these results has received funding from the National Science Foundation of China (Grant nos. 51475246, 51277098, and 51075215), the Research Innovation Program for College Graduates of Jiangsu Province (Grant no. KYLX15_0725), and the Natural Science Foundation of Jiangsu Province of China (Grant no. BK20131402).

References

[1] S.-B. Choi, H.-S. Lee, and Y.-P. Park, "H_∞ control performance of a full-vehicle suspension featuring magneto-rheological dampers," *Vehicle System Dynamics*, vol. 38, no. 5, pp. 341–360, 2002.

[2] E. R. Wang, X. Q. Ma, S. Rakheja, and C. Y. Su, "Modeling hysteretic characteristics of an MR-fluid damper," *Journal of Automobile Engineering*, vol. 217, pp. 537–550, 2003.

[3] R. Li, M. Yu, W. Chen, C. Liao, and X. Dong, "Control of automotive suspensions vibration via magneto rheological damper," *Chinese Journal of Mechanical Engineering*, vol. 41, no. 6, pp. 128–132, 2005.

[4] E. R. Wang, L. Ying, W. J. Wang, S. Rakheja, and C. Y. Su, "Semi-active control of vehicle suspension with magneto-rheological dampers: part I—controller synthesis and evaluation," *Chinese Journal of Mechanical Engineering*, vol. 21, no. 1, pp. 13–19, 2008.

[5] J. J. Lozoya-Santos, R. Morales-Menendez, and R. A. Mendoza, "Control of an automotive semi-active suspension," *Mathematical Problems in Engineering*, vol. 2012, Article ID 218106, 21 pages, 2012.

[6] J. O. Pedro, M. Dangor, O. A. Dahunsi, and M. M. Ali, "Differential evolution-based PID control of nonlinear full-car electrohydraulic suspensions," *Mathematical Problems in Engineering*, vol. 2013, Article ID 261582, 13 pages, 2013.

[7] H. Zhang, E. Wang, F. Min, R. Subash, and C. Su, "Skyhook-based semi-active control of full-vehicle suspension with magneto-rheological dampers," *Chinese Journal of Mechanical Engineering (English Edition)*, vol. 26, no. 3, pp. 498–505, 2013.

[8] M. Canale, M. Milanese, and C. Novara, "Semi-active suspension control using 'fast' model-predictive techniques," *IEEE Transactions on Control Systems Technology*, vol. 14, no. 6, pp. 1034–1046, 2006.

[9] J. Swevers, C. Lauwerys, B. Vandersmissen, M. Maes, K. Reybrouck, and P. Sas, "A model-free control structure for the on-line tuning of the semi-active suspension of a passenger car," *Mechanical Systems and Signal Processing*, vol. 21, no. 3, pp. 1422–1436, 2007.

[10] S. M. Savaresi and C. Spelta, "A single-sensor control strategy for semi-active suspensions," *IEEE Transactions on Control Systems Technology*, vol. 17, no. 1, pp. 143–152, 2009.

[11] H. J. Gao, W. C. Sun, and P. Shi, "Robust sampled-data H_∞ control for vehicle active suspension systems," *IEEE Transactions on Control Systems Technology*, vol. 18, no. 1, pp. 238–245, 2010.

[12] C. Gohrle, A. Schindler, A. Wagner, and O. Sawodny, "Design and vehicle implementation of preview active suspension controllers," *IEEE Transactions on Control Systems Technology*, vol. 22, no. 3, pp. 1135–1142, 2014.

[13] W. C. Sun, H. J. Gao, and B. Yao, "Adaptive robust vibration control of full-car active suspensions with electrohydraulic actuators," *IEEE Transactions on Control Systems Technology*, vol. 21, no. 6, pp. 2417–2422, 2013.

[14] T. Li, C.-J. Huang, and C.-C. Chen, "Almost disturbance decoupling control of MIMO nonlinear system subject to feedback linearization and a feedforward neural network: application to half-car active suspension system," *International Journal of Automotive Technology*, vol. 11, no. 4, pp. 581–592, 2010.

[15] M. C. Smith and F.-C. Wang, "Controller parameterization for disturbance response decoupling: application to vehicle active suspension control," *IEEE Transactions on Control Systems Technology*, vol. 10, no. 3, pp. 393–407, 2002.

[16] L. Wu and X. Wen, "A research on the decoupling of a 6 DOF half vehicle suspension and its hierarchical vibration control," *Automotive Engineering*, vol. 32, no. 2, pp. 148–167, 2010 (Chinese).

[17] X. M. Dong, M. Yu, W. M. Chen, C. Liao, S. Huang, and Z. Li, "Research on application of human-like intelligent control used to vehicle magneto-rheological semi-active suspension," *China Mechanical Engineering*, vol. 18, no. 7, pp. 764–769, 2007.

[18] S. Diop and M. Lakehal-Ayat, "More on a decoupled control model of a vehicle suspension system," in *Proceedings of the IEEE International Symposium on Industrial Electronics (ISIE '05)*, pp. 405–410, IEEE, Dubrovnik, Croatia, June 2005.

[19] M. Lakehal-Ayat, S. Diop, and E. Fenaux, "An improved active suspension yaw rate control," in *Proceedings of the American Control Conference*, pp. 863–868, Anchorage, Alaska, USA, May 2002.

[20] D. P. Cao, S. Rakheja, and C.-Y. Su, "Roll- and pitch-plane coupled hydro-pneumatic suspension part 1: feasibility analysis and suspension properties," *Vehicle System Dynamics*, vol. 48, no. 3, pp. 361–386, 2010.

[21] B. L. Gu, *BOSCH Automotive Handbook*, Beijing Institute of Technology Press, Beijing, China, 5th edition, 2004 (Chinese).

[22] E. R. Wang, H. L. Zhang, F. H. Min, W. Yan, and M. Y. Huang, "A control scheme of new semi-active vehicle suspension with dual controllable dampers," Patent D ZL 201210508961.4, State Intellectual Property Office of P.R.C: Patent for Invention, March 2013.

[23] E. Atlas, M. I. Erdoğan, O. B. Ertin et al., "Hardware-in-the-loop test platform design for UAV applications," *Applied Mechanics and Materials*, vol. 789-790, pp. 681–687, 2015.

[24] H. Zhang, N. Zhang, F. Min, W. Yan, and E. Wang, "Bifurcations and chaos of a vibration isolation system with magneto-rheological damper," *AIP Advances*, vol. 6, Article ID 035310, 11 pages, 2016.

[25] W. J. Wang, L. Ying, and E. R. Wang, "Comparison on hysteresis models of controllable magneto-rheological damper," *Journal of Mechanical Engineering*, vol. 45, no. 9, pp. 100–108, 2009.